*Materials Research*. 2017; 20(2): 538-542
DOI: http://dx.doi.org/10.1590/1980-5373-MR-2016-0606


# Structural Evolution and Electrical Properties of $BaTiO_3$ Doped with $Gd^{3+}$

***Juan Pablo Hernández Lara[a], Miguel Pérez Labra[a]*, Francisco Raúl Barrientos Hernández[a], Jose Antonio Romero Serrano[b], Erika Osiris Ávila Dávila[c], Pandiyan Thangarasu[d], Aurelio Hernández Ramirez[b]***

*[a] Academic Area of Earth Sciences and Materials, Autonomous University of Hidalgo State, Road Pachuca- Tulancingo Km 4.5 Mineral de la Reforma Zip Code 42184, Hidalgo México*
*[b] Metallurgy and Materials Department, ESIQIE-IPN. UPALM, Zacatenco, Zip Code 07738, México*
*[c] Mechanical Engineering Department, Technological Institute of Pachuca, Road México-Pachuca km. 87.5 Pachuca de Soto Zip Code 42080, Hidalgo, México*
*[d] Circuito interior s/n Facultad de Química Edif. F Lab. 114 Ciudad Universitaria UNAM México D. F. Zip Code 04510*

Received: August 19, 2016; Revised: January 10, 2017; Accepted: February 02, 2017

$BaTiO_3$ doped with $Gd^{3+}$ ($Ba_{1-x}Gd_xTi_{1-x/4}O_3$) was synthesized using the solid-state reaction method with x = 0.001, 0.003, 0.005, 0.01, 0.05, 0.1, 0.15, 0.20, 0.25, 0.30, and 0.35 $Gd^{3+}$ (wt. %). The powders were decarbonated at 900 °C and sintered at 1400 °C for 8 hours. The tetragonality of the synthesized $Gd^{3+}$-doped $BaTiO_3$ particles was analyzed. XRD patterns and Raman spectra revealed that the crystal phase of the obtained particles was predominately tetragonal $BaTiO_3$; the intensity of the Raman bands at 205 $cm^{-1}$, 265 $cm^{-1}$, and 304 $cm^{-1}$ decreased when $Gd^{3+}$ was increased. A secondary phase ($Gd_2Ti_2O_7$) was found when the $Gd^{3+}$ content was higher than 0.15 wt. %. The capacitance of the sintering pellets was measured at 1 kHz; these values were used to calculate the relative permittivity, the maximum permittivity values were recorded for the samples with x = 0.001, 0.005, and 0.1.

**Keywords:** *$Gd^{3+}$, $BaTiO_3$, Dielectric*

## 1. Introduction

$BaTiO_3$ (BT) is a ferroelectric material with a characteristic tetragonal distortion of the cubic perovskite structure. The ferroelectric (tetragonal) phase gets converted to paraelectric (cubic) phase at the Curie temperature (Tc) at ~ 120 °C for single-crystals. However, Tc for polycrystalline BT will shift to lower values due to the metastable cubic phase at temperatures below 120°C. The ferroelectric distortion is facilitated by the large size of the Ba cation. The ferroelectric property owes its origin to a displacement of the Ti atoms and the effect is very sensitive to interatomic distances (lattice parameter). Among the most important properties that can be presented to highlight both its chemical and mechanical stability is its ferroelectric properties at room temperature considering its use as a polycrystalline ceramic[1]. BT is widely used in the manufacture of piezoelectric devices, electro-optical elements, ceramic capacitors, and resistors due to its high dielectric constant and semiconducting properties when they are modified using aliovalent or isovalent dopants[2]. The high dielectric constant allows smaller capacitive components, thus offering an opportunity to reduce the size of electronic devices[3,4]. The understanding of how these particular crystalline structures evolve from the tetragonal perovskite structure might provide a way to engineer more compounds with hexagonal structure.

It is known that an appropriate amount of doping into the BT can improve the structural, optical, and electrical properties of the system[4-7]. Doping has been studied by several authors[7,8] and it was shown, for example, that the positive temperature coefficient of resistivity (PTCR) effect in $BaTiO_3$ doped with donors (when the substitution occurs at Ba sites) can be significantly increased by adding small amounts of dopants. This additional doping leads to an increase of the ρmax/ρmin ratio (ρ is the electric resistivity) which is the most important feature to be applied. Even more, the dopants can influence the temperature of the ferroelectric phase transition (Tc). The investigation of the dopants' effects plays a decisive role in understanding the nature and in optimizing the properties of $BaTiO_3$ ceramics. Manjit Borah[9] report the structural, optical and dielectric characterization of solid state derived, pseudo-cubic nanoscale barium titanates with gadolinium ($Gd^{3+}$) as substitutional dopant. It was found that the dielectric constant showed a decreasing tendency with doping content when the Gd-doping level was varied between 0 –7 %.

As a lanthanide element, Gd exhibits unusual metallurgical properties, apart from its significant use in magnetic resonance imaging (MRI). The inclusion of Gd into the pseudo-cubic host lattice of BT is rarely found in the literature. The main goal of this work was the investigation of structural evolution and electrical properties of $BaTiO_3$ ceramics doped with

* e-mail: miguelabra@hotmail.com

$Gd^{3+}$ varied within 0.001, - 0.35 $Gd^{3+}$ (wt. %) using the solid-state reaction method.

This method is an important technique in the preparation of polycrystalline solids. A solid state reaction, also called dry reaction mixture of oxides, is a chemical reaction in which no solvents are used. The advantages of this method (compared to other techniques) are mainly economic and, hence, large scale production is frequently based on solid-state reactions of mixed powders.

## 2. Experimental

Samples of BT doped with $Gd^{3+}$ were prepared according to the formula $Ba_{1-x}Gd_xTi_{1-x/4}O_3$ using the solid-state reaction method by grinding $BaCO_3$ (Sigma-Aldrich, CAS No. 513-77-9, 99.9%), $TiO_2$ (Sigma-Aldrich, CAS No. 13463-67-7, 99.9%), and $Gd_2O_3$ (Sigma-Aldrich, CAS No. 278513-25G, 99.9%) in an agate mortar, with acetone as a control medium and x = 0.001, 0.003, 0.005, 0.01, 0.05, 0.1, 0.15, 0.20, 0.25, 0.30, 0.35 $Gd^{3+}$ (wt. %)

The precursor powders ($BaCO_3$, $TiO_2$ and $Gd_2O_3$) were dried at 200 °C, before weighing. The powder mixture was placed in an alumina boat then decarbonated at 900 °C overnight, and later was reground for 10 min in an agate mortar. After that, the powder mixtures were sintered in a platinum crucible at 1400 °C for 8 hours using a muffle furnace (Thermolyne model 46200). The purity of the products was monitored by X-ray diffraction (Diffractometer Inel Equinox 2000 Cu Kα, radiation of λ =0.15418nm).

Once the powders were obtained for each composition pellets were manufactured for each composition. The powder mixtures were regrounded again and later compacted using uniaxial pressing at 250 MPa in an 8-mm stainless steel die to produce green pellets of 3 mm thickness. The pellets were sintered at 1400 °C for 5 hours in air atmosphere with heating and cooling rates of 5 °C/min. They were grounded with silicon carbide abrasive paper, polished with slurry of alumina and later cleaned in an ultrasonic bath. The morphology studies were performed in a JEOL 6300 SEM, 15kV, WD 8.1mm. Electrical measurements were performed on an LC Meter Analyzer (ELC-3133A LCM Escort), at 1 KHz. Additionally, Raman studies were carried out for each powder samples using a Perkin Elmer Spectrum Gx spectrophotometer, (Überlingen, Germany), with neodymium laser (1064 nm) excitation.

## 3. Results and discussion

### *3.1 X-Ray diffraction*

Owing to the difference in effective ionic radii between gadolinium and titanium ($r(Gd^{3+})$ = 1.00 Å, $r(Ti^{4+})$ = 0.605 Å)[10] the lattice will expand to some extent.

This may be one of the reasons why the XRD reflections shift to lower angles (Figure 1 and Figure 2) at 2θ = 65.7 and $x \geq 0.15$ after sintering at 1400 °C, this is similar to reported by Barrientos et al.[11].

It can be seen from Figure 1 that the diffractograms show a double peak at $2\theta \approx 45$, indicating the presence of tetragonal ferroelectric phase (JCPDS 050626) for the diffractograms when $Gd^{3+}$ content $0.001 \leq x \leq 0.3$. This phase disappears for the sample with $Gd^{3+}$ content x = 0.35, however, a secondary phase ($Gd_2Ti_2O_7$) (JCPDS 731698) was found when the $Gd^{3+}$ content was higher than 0.15, as observed in the peak $2\theta \approx 32$. The $Gd_2Ti_2O_7$ phase was identified for $0.001 \leq x \leq 0.35$. Parida et al.[12] studied a series of $Gd_2Ti_2O_7/GdCrO_3$ composites prepared by the solid state combustion method using $Gd(NO_3)_3$, $TiO_2$, $Cr_2O_3$ as metal sources and urea as a fuel. Parida et al. have found the $Gd_2Ti_2O_7$ phase, whereby the main peaks matched the secondary phase found in this work.

### *3.2 Raman Spectroscopy*

Raman spectroscopy (RS) was used to study the phase transition of $Gd^{3+}$-doped $BaTiO_3$ ceramics. RS is a spectroscopic technique used to observe vibrational, rotational, and other low-frequency modes in a system[7]. Figure 3 shows the Raman spectra for $BaTiO_3$ doped with several $Gd^{3+}$ concentrations prepared by the solid-state reaction. The graphs show the characteristic Raman peaks at room temperature of $BaTiO_3$[8,13,14] located at 205 $cm^{-1}$ (E(TO + LO), A1(LO)), 265 $cm^{-1}$ (A1(TO)), 304 $cm^{-1}$ (B1, E(TO + LO)), 513 $cm^{-1}$ (A1(TO), E(TO)) and 717 $cm^{-1}$ (A1(LO), E(LO)). Similar bands were observed in $BaTiO_3$ based ceramics by Suchanicz et al.[13] and Pokorny et al.[14]. An extra band was observed at 833 $cm^{-1}$ whose intensity was proportional to the $Gd^{3+}$ concentration. This high-frequency mode (above 700 $cm^{-1}$) can be caused by the vibrations resulting from the shift of oxygen and also correlated to present of oxygen vacancies, Suchanicz et al.[15]. On the other hand, was observed that this extra band occurs when $Gd^{3+}$ content was Gd $0.01 \leq x \leq 0.35$, which was coherent with the appearance of the secondary phase $Gd_2Ti_2O_7$ (see Figure 1). Barrientos et al.[11], in a study of the structural evolution of hexagonal phase $Ba_8Ti_3Nb_4O_{24}$ by adding $Nb_2O_5$ to perovskite $BaTiO_3$, associated the appearance of an extra band around 743 $cm^{-1}$ and 830 $cm^{-1}$ with the presence of the secondary phase $Ba_8Ti_3Nb_4O_{24}$, equally identified by XRD. When the dopant concentration in $BaTiO_3$ is enough to cross through the tetragonal–cubic phase transition point, all the active Raman modes in the tetragonal phase (P4 mm) are inactive in the perfect cubic phase (Pm3 m) according to forbidden Raman selection rules. However, the broad A1 (TO) band at 513 $cm^{-1}$ persisted into the cubic phase above Tc, which was attributed to intrinsic disorder in the cubic phase, and it becomes broad and weak with increasing $Gd^{3+}$ content[16]. A dramatic change at low frequencies was found with increasing dopant content. The

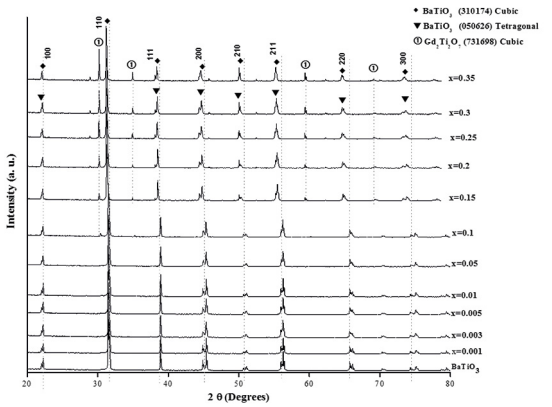


**Figure 1:** XRD diffractograms for $Ba_{1-x}Gd_xTi_{1-x/4}O_3$ powders sintered at 1400 °C for 8 h for different values of x.

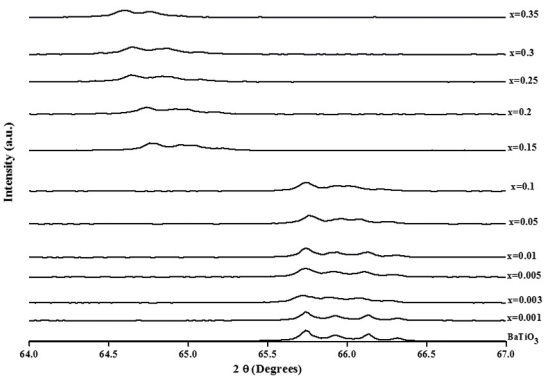


**Figure 2:** XRD diffractograms for $Ba_{1-x}Gd_xTi_{1-x/4}O_3$ powders sintered at 1400 °C for 8 h for different values of x. Zoom at 64–67°

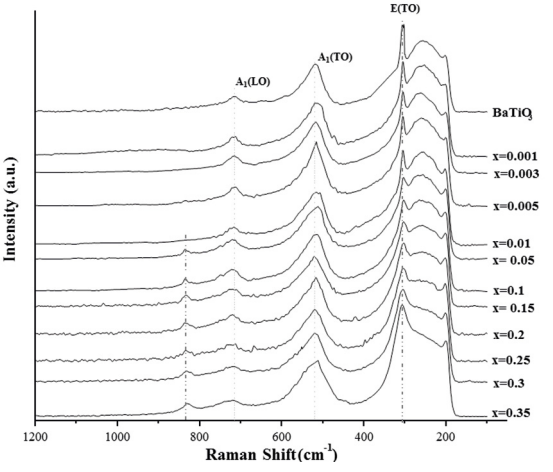


**Figure 3:** Raman spectra of powders sintered at 1400 °C, $0 \leq x \leq 0.3$.

Raman peak around 304 $cm^{-1}$ showed a decrease in intensity. This diminution was attributed to the decrease of tetragonality of BT ceramics. The phase transformation was observed in DRX results when $Gd^{3+}$ content was $x \geq 0.35$ (Figure 1) and dielectric measurements.

## *3.3 Electric Properties*

Platinum paste was painted on opposite surfaces of the pellets to form electrodes; a thin platinum strip was applied to the platinum electrodes to act as a contact. Figure 4 shows the results of relative permittivity (k) obtained at 1 kHz for the compositions prepared in the range of $0 \leq x \leq 0.35$. The maximum permittivity values were recorded for the samples with x = 0.001, 0.005, and 0.1. It has been reported[9] that the dielectric constant showed a decreasing tendency with doping content and with increasing frequency for pseudo-cubic nanometric barium titanate doped with gadolinium ($Gd^{3+}$) where the doping level was varied between 0–7 %. However, it was also determined that in the low-frequency region, the loss tangent (tan δ), which is the combined result of orientational polarization and electrical conduction, was found to be quite high in the doped samples as compared to their un-doped counterpart. In this study only results obtained at 1 kHz were reported.

The maximum value of k was registered for the sample with x = 0.001 (10474.35). The main Curie peak shift from 112 °C to 76 °C indicated that the cubic phase was becoming more stable. Furthermore, the compositions x = 0.25, x = 0.2, x = 0.3 and x = 0.35 showed Curie temperature values of 83 to 65 °C with permittivity values of 5319, 4364, 3529, and 3174 respectively. However, the low intensity and width of the peaks indicated a mixture of phases.

## *3.4 Morphology and microstructure*

Figure 5 shows SEM- EDS images of $Gd^{3+}$-doped $BaTiO_3$ sintered at 1400 °C for the samples with x = 0.15 and x = 0.35, which consisted of rounded grains with a wide grain-size distribution visually observed from SEM images; grain sizes of 1.8– 8.4 mm for x = 0.15 (Figure 5a), and 3.2–11.2 mm for x = 0.35 (Figure 5b). The presence of Gd can be observed in the EDS spectrum. The SEM images of the samples indicated that $Gd^{3+}$ does not drastically influence the microstructure.

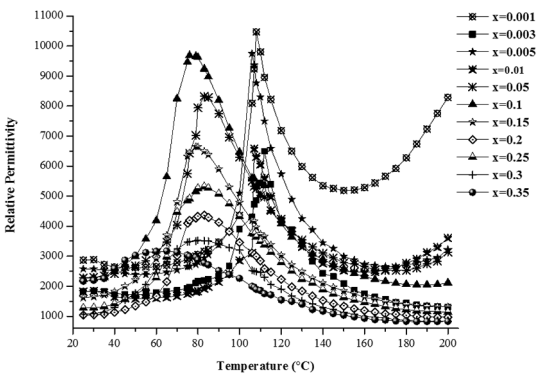


**Figure 4:** Relative permittivity at 1 kHz as a function of temperature capacitors prepared from $Ba_{1-x}Gd_xTi_{1-x/4}O_3$ with $0 \leq x \leq 0.35$

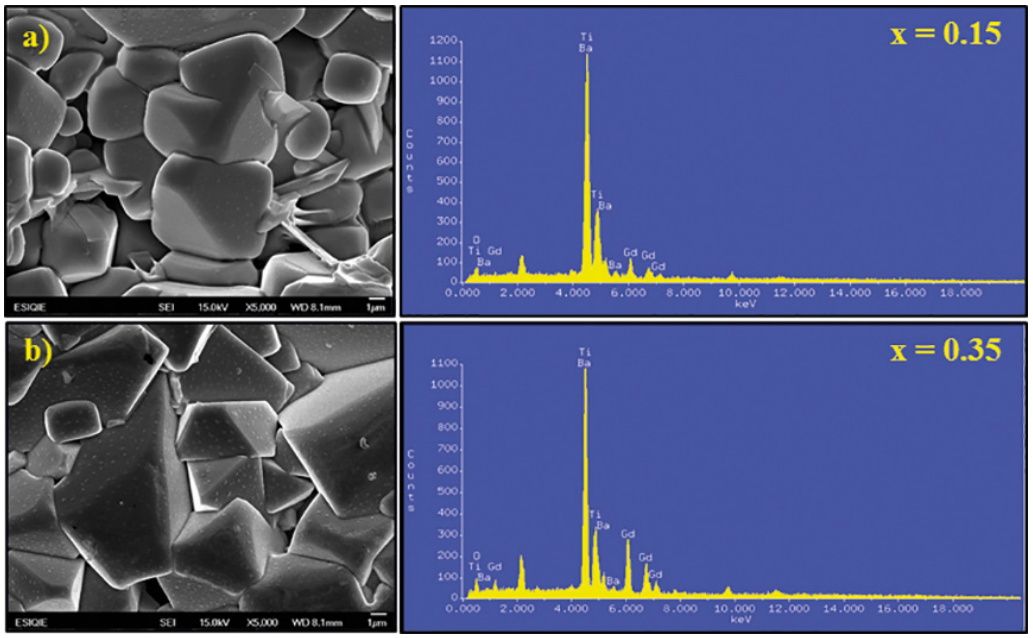


**Figure 5:** SEM-EDS micrographs of $BaTiO_3$, doped with different $Gd^{3+}$. a) x= 0.15, and b) x= 0.35.

All of the samples revealed comparable grain sizes. A relatively homogeneous microstructure with higher amounts of inter-granular porosity was also observed; this may due to the behavior of $Gd^{3+}$ in the $BaTiO_3$ ceramics. In the detailed image (Figure 6), this characteristic can be observed[11].

A summary of semiquantitative compositions obtained by SEM-EDS for all samples is shown in Table 1. The EDS investigations showed that the ceramics $BaTiO_3$ + x wt. % $Gd^{3+}$ ($0.001 \leq x \leq 0.35$) contained Ba, Ti, O, and Gd elements near their surfaces. No other elements were detected.

It was noted that the content of Gd increased as x increased. On the contrary, with x content increasing, the Ba and Ti contents decreased. This can be explained by the amphoteric behavior of $BaTiO_3$ [17], e.g. $BaTiO_3$ behaves as an acceptor when the Ti site is substituted or as donor when the substitution occurs at the Ba site.

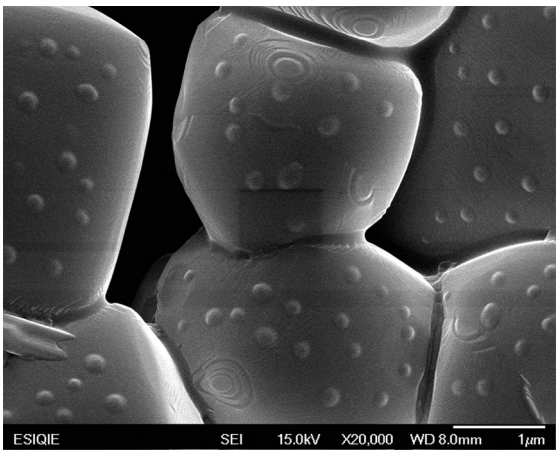


**Figure 6:** SEM micrograph detail of $Gd^{3+}$ doped $BaTiO_3$, x = 0.15.

**Table 1:** Semiquantitative chemical compositions (SEM-EDS) of powders sintered at 1400 °C, $0 \leq x \leq 0.35$ (wt.%).

| Sample | Wt. (%) | | | |
|---|---|---|---|---|
| | Ba | Ti | O | Gd |
| $BaTiO_3$ | 68.46 | 25.31 | 6.22 | 0 |
| x = 0.001 | 65.64 | 23.98 | 10.31 | 0.07 |
| x = 0.003 | 61.41 | 21.93 | 16.41 | 0.25 |
| x = 0.005 | 61.87 | 20.13 | 17.66 | 0.34 |
| x = 0.010 | 58.03 | 20.51 | 20.74 | 0.72 |
| x = 0.050 | 54.38 | 21.15 | 21.75 | 2.72 |
| x = 0.100 | 50.81 | 22.74 | 13.03 | 13.42 |
| x = 0.150 | 48.68 | 19.33 | 15.85 | 16.14 |
| x = 0.200 | 46.64 | 19.22 | 9.83 | 24.31 |
| x = 0.250 | 41.01 | 19.14 | 12.83 | 27.02 |
| x = 0.300 | 38.88 | 19.01 | 12.37 | 29.74 |
| x = 0.350 | 36.02 | 19.11 | 10.92 | 33.95 |

Yongping et al.[17] reported that the thermodynamic conditions, such as the partial pressure of oxygen in the sintering atmosphere and temperature, play an important part in the distribution of rare earth elements with amphoteric behavior in the A or B sites of $BaTiO_3$[18,19].

## 4. Conclusions

$BaTiO_3$ doped with $Gd^{3+}$ ($Ba_{1-x}Gd_xTi_{1-x/4}O_3$) with x = 0.001, 0.003, 0.005, 0.01, 0.05, 0.1, 0.15, 0.20, 0.25, 0.30, and 0.35 $Gd^{3+}$ (wt. %) was investigated by XRD, RS

and electric measurements. A double peak at $2\theta \approx 45$ was confirmed by XRD, indicating the presence of a tetragonal ferroelectric phase for the diffractograms when the $Gd^{3+}$ content was $0.001 \leq x \leq 0.3$. This phase disappeared for the sample with $Gd^{3+}$ content $x = 0.35$. A secondary phase ($Gd_2Ti_2O_7$) was found when the $Gd^{3+}$ content was higher than 0.15, as was observed in XRD at $2\theta \approx 32$. $Gd_2Ti_2O_7$ phase was identified for $0.001 \leq x \leq 0.35$. The Raman results showed the characteristic Raman peaks of the tetragonal ferroelectric phase of $BaTiO_3$ located at 205 $cm^{-1}$ (E(TO + LO), A1(LO)), 265 $cm^{-1}$ (A1(TO)), 304 $cm^{-1}$ (B1, E(TO + LO)), 513 $cm^{-1}$ (A1(TO), E(TO)), and 717 $cm^{-1}$ (A1(LO), E(LO)). The maximum permittivity values were recorded for the samples with $x = 0.001$, 0.005, and 0.1. The extra band observed $0.01 \leq x \leq 0.35$ (833 $cm^{-1}$) was coherent with the appearance of the secondary phase ($Gd_2Ti_2O_7$) observed equally by DRX.

The incorporation of $Gd^{3+}$ ions into the BT system could greatly manifest dielectric properties and can find immense scope in electronic elements including ceramic capacitors.

## 5. Acknowledgment

The authors are grateful to CONACyT-México for the financial support.

## 6. References

1. Jona F, Shirane G. *Ferroelectric Crystals*. Mineola: Dover Publications; 1993.

2. Rae A, Chu M, Ganine V. Barium Titanate: Past, Present and Future. In: Nair KM, Bhalla AS, eds. *Dielectric Ceramic Materials*. Westerville: The American Ceramic Society; 1999.

3. Jin S, Xia H, Zhang Y, Guo J, Xu J. Synthesis of $CaCu_3Ti_4O_{12}$ ceramic via a sol-gel method. *Materials Letters*. 2007;61(6):1404-1407.

4. Ali AI, Ahn CW, Kim YS. Enhancement of piezoelectric and ferroelectric properties of $BaTiO_3$ ceramics by aluminum doping. *Ceramics International*. 2013;39(6): 6623-6629.

5. Abdelmoula N, Khemakhem H, Simon A, Maglione M. Structure refinement, dielectric, pyroelectric and Raman characterizations of $Ba_{1-x}La_{x(1-y)/2}Eu_{xy/2}Na_{x/2}TiO_3$ solid solution. *Journal of Solid State Chemistry*. 2006;179(12):4011-4019.

6. Yang Y, Liu K, Liu X, Liu G, Xia C, He Z, et al. Electrical properties and microstructures of (Zn and Nb) co-doped $BaTiO_3$ ceramics prepared by microwave sintering. *Ceramics International*. 2016;42(6):7877-7882.

7. Ueoka H. The doping effects of transition elements on the PTC anomaly of semiconductive ferroelectric ceramics. *Ferroelectrics*. 1974;7(1):351-353.

8. Hiroshi Ikushima and Shigeru Hayakawa. Electrical Properties of Ag-Doped Barium Titanate Ceramics. *Japanese Journal of Applied Physics.* 1965; 4 (5): 328-336

9. Borah M, Mohanta D. Effect of $Gd^{3+}$ doping on structural, optical and frequency-dependent dielectric response properties of pseudo-cubic $BaTiO_3$ nanostructures. *Applied Physics A*. 2014;115(3):1057-1067.

10. Shannon RD. Revised effective ionic radii and systematic studies of interatomic distances in halides and chalcogenides. *Acta Crystallographica Section A*. 1976;32(5):751-767.

11. Hernández FRB, Hernández IAL, Yáñez CG, Flores A, Sierra RC, Labra MP. Structural evolution of $Ba_8Ti_3Nb_4O_{24}$ from $BaTiO_3$ using a series of $Ba(Ti_{1-5x}Nb_{4x})O_3$ solid solutions. *Journal of Alloys and Compounds*. 2014;583:587-592.

12. Parida KM, Nashim A, Mahanta SK. Visible-light driven $Gd_2Ti_2O_7/GdCrO_3$ composite for hydrogen evolution. *Dalton Transactions*. 2011;40(48):12839-12845.

13. Suchanicz J, Świerczek K, Nogas-Ćwikiel E, Konieczny K, Sitko D. $PbMg_{1/3}Nb_{2/3}O_3$-doping effects on structural, thermal, Raman, dielectric and ferroelectric properties of $BaTiO_3$ ceramics. *Journal of the European Ceramic Society*. 2015;35(6):1777-1783.

14. Pokorný J, Pasha UM, Ben L, Thakur OP, Sinclair DC, Reaney IM. Use of Raman spectroscopy to determine the site occupancy of dopants in $BaTiO_3$. *Journal of Applied Physics*. 2011;109(11):114110.

15. Suchanicz J, Klimkowski G, Karpierz M, Lewczuk U, Faszczowy I, Pękala A, et al. Influence of Compressive Stress on Dielectric and Ferroelectric Properties of the$(Na_{0.5}Bi_{0.5})_{0.7}Sr_{0.3}TiO_3$ Ceramics. *IOP Conference Series: Materials Science and Engineering*. 2013;49(1):012038.

16. Gardiner DJ, Graves PR, eds. *Practical Raman Spectroscopy*. Berlin, Heidelberg, New York: Springer-Velarg; 1989.

17. Yongping P, Wenhu Y, Shoutian C. Influence of rare earths on electric properties and microstructure of barium titanate ceramics. *Journal of Rare Earths*. 2005;25(Suppl 1):154-157.

18. Zhi J, Chen A, Zhi Y, Vilarinho PM, Baptista JL. Incorporation of Yttrium in Barium Titanate Ceramics. *Journal of the American Ceramic Society*. 1999;83(5):1345-1348.

19. Tsur Y, Dunbar TD, Randall CA. Crystal and Defect Chemistry of Rare Earth Cations in $BaTiO_3$. *Journal of Electroceramics*. 2001;7(1):25-34.